Phytochemistry 92 (2013) 113–121

Contents lists available at SciVerse ScienceDirect

Phytochemistry

journal homepage: www.elsevier.com/locate/phytochem

Polyphenols from the bark of *Rhus verniciflua* and their biological evaluation on antitumor and anti-inflammatory activities

Ki Hyun Kim [a], Eunjung Moon [b], Sang Un Choi [c], Sun Yeou Kim [d], Kang Ro Lee [e,*]

[a] Department of Chemistry and Chemical Biology, Harvard University, 12 Oxford Street, Cambridge, MA 02138, USA
[b] Graduate School of East-West Medical Science, Kyung Hee University Global Campus, #1732 Deogyeong-daero, Giheung-gu, Yongin, Gyeonggi-do 446-701, Republic of Korea
[c] Korea Research Institute of Chemical Technology, Teajeon 305-600, Republic of Korea
[d] College of Pharmacy, Gachon University, #191 Hambakmoero, Yeonsu-gu, Incheon 406-799, Republic of Korea
[e] Natural Products Laboratory, School of Pharmacy, Sungkyunkwan University, Suwon 440-746, Republic of Korea

ARTICLE INFO

Article history:
Received 13 November 2012
Received in revised form 27 February 2013
Accepted 8 May 2013
Available online 8 June 2013

Keywords:
Rhus verniciflua
Anacardiaceae
Polyphenols
Rhusopolyphenols
Antitumor
Anti-inflammation

ABSTRACT

Bioassay-guided fractionation and chemical investigation of the extract of *Rhus verniciflua* bark resulted in the identification of six polyphenols, rhusopolyphenols A–F (**1**–**6**), together with four known compounds including (2*R*,3*S*,10*S*)-7,8,9,13-tetrahydroxy-2-(3,4-dihydroxyphenyl)-2,3-*trans*-3,4-*cis*-2,3,10-trihydrobenzopyrano[3,4-*c*]-2-benzopyran-1-one (**7**), peapolyphenol C (**8**), cilicione-b (**9**) and (α*R*)-α,3,4,2′,4′-pentahydroxydihydrochalcone (**10**). The structures of these polyphenols were elucidated by spectroscopic analysis, including 1D and 2D NMR, and HR-ESIMS, and their absolute configurations were further confirmed by a combination of chemical methods and CD data analysis. All isolates were evaluated for their antiproliferative activities against four human tumor cell lines (A549, SK-OV-3, SK-MEL-2, and HCT-15), and compounds **4**–**6**, **9** and **10** showed antiproliferative activity against the tested cells, with IC_{50} values of 3.31–18.51 μM. On the basis of the expanded understanding that inflammation is a crucial cause of tumor progression, the anti-inflammatory activities of these compounds were determined by measuring nitric oxide (NO) levels in the medium of murine microglia BV-2 cells. Compounds **5** and **10** significantly inhibited NO production in lipopolysaccharide (LPS)-stimulated murine microglia BV-2 cells with IC_{50} values of 28.90 and 12.70 μM, respectively.

1. Introduction

Polyphenols constitute one of the most ubiquitous groups of plant metabolites that are utilized as important components in both human and animal diets (Bravo, 1998). For decades, plant polyphenols have interested scientists because they are essential to plant growth and reproduction and some can also provide plants with resistance to pathogens and predators by acting as phytoalexins (Bravo, 1998). Polyphenols exhibit a wide range of biological effects as a consequence of their antioxidant properties such as antithrombotic, anti-inflammatory, and antimicrobial effects (Gerritsen et al., 1995; Muldoon and Kritchevsky, 1996; Chung et al., 1998). Several studies have shown that polyphenols have anticarcinogenic and antimutagenic effects by inactivating carcinogens and inhibiting expression of mutant genes as well as by inhibiting the activity of enzymes involved in activation of procarcinogens (Hour et al., 1999; Dai and Mumper, 2010; Coates et al., 2007). In the course of this study to search for bioactive metabolites from Korean medicinal sources, it was found that the EtOH extract of *Rhus verniciflua* bark exhibited considerable cytotoxicity against A549, SK-OV-3, SK-MEL-2, and HCT-15 cell lines during the screening procedures employed.

Medicinal plants have been used to treat various diseases since ancient times. *R. verniciflua* (Anacardiaceae) has been used in traditional Korean medicine as a herbal therapy for treating abdominal disorders, inflammatory diseases, and various cancers in South Korea (Lee et al., 2010). The medical use of this plant has been limited because of its toxic allergen, urushiol, which causes severe dermatitis. After boiling the plant with other foods such as chicken and duck to alleviate toxicity, the cooked herb is eaten to acquire its useful effects (Lee et al., 2010). In the studies of biological activities of this herb by a number of investigators, the extract of this plant exhibited anticancer and antiproliferative effects in various cancer cell lines (Lee et al., 2003, 2010; Kook et al., 2007; Son et al., 2005; Samoszuk et al., 2005), which has also been confirmed by our screening tests showing that the *R. verniciflua* EtOH extract had excellent cytotoxic activity against the above-mentioned tumor cells using a sulforhodamine B (SRB) bioassay. But, few reports have emphasized the active constituents responsible for the

* Corresponding author. Address: Natural Products Laboratory, School of Pharmacy, Sungkyunkwan University, 300 Chonchon-dong, Jangan-ku, Suwon 440-746, Republic of Korea. Tel.: +82 31 290 7710; fax: +82 31 290 7730.
E-mail address: krlee@skku.ac.kr (K.R. Lee).

0031-9422/$ - see front matter © 2013 Elsevier Ltd. All rights reserved.
http://dx.doi.org/10.1016/j.phytochem.2013.05.005

antitumor effect in this plant. Therefore, in the present study, focus was placed upon *R. verniciflua* constituents with antitumor activity, which will be potentially helpful to develop novel drugs and functional foods. Bioassay-guided fractionation and chemical investigation of the EtOH extract of the *R. verniciflua* bark resulted in isolating and identifying six new polyphenols (**1**–**6**), together with four known analogs (**7**–**10**). Herein, we describe the isolation and structural elucidation of these isolates (**1**–**10**) and the biological evaluation of antitumor and anti-inflammatory activities.

2. Results and discussion

Dried *R. verniciflua* bark in H_2O was fermented by *Aspergillus oryzae* for 35 h at 30 °C to augment diversified active constituents and remove the toxic constituent urushiol, which is an oily organic allergen found in plants of the family Anacardiaceae (Kim et al., 2011). The fermented material was extracted with H_2O under reflux, and the extract was further extracted with EtOH to afford a crude EtOH extract. The EtOH extract was successively fractionated by octadecylsilyl (ODS) chromatography, and the resulting active fractions were purified by ODS HPLC to yield six new polyphenols (**1**–**6**, Fig. 1), and four known analogs (**7**–**10**).

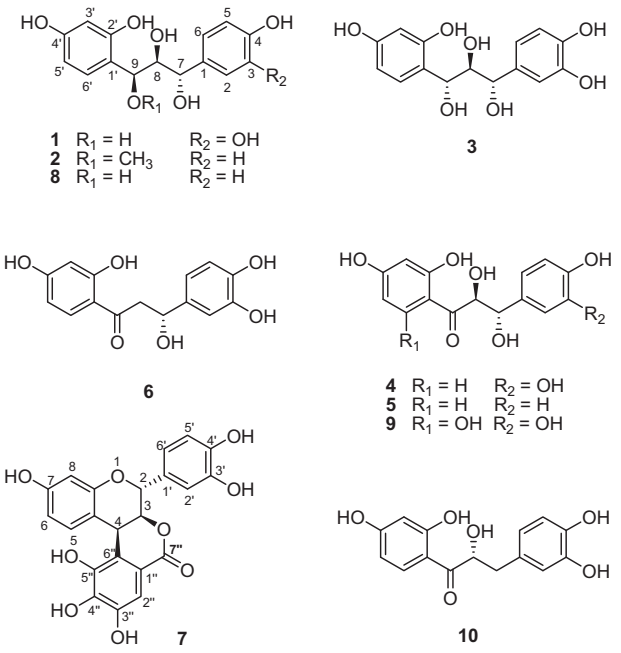

Fig. 1. Chemical structures of the isolated compounds (**1**–**10**).

Compound **1** was obtained as a colorless gum. The molecular formula was established as $C_{15}H_{16}O_7$, based on HR-ESIMS (*m/z* 331.0797 $[M+Na]^+$, calcd. for $C_{15}H_{16}NaO_7$, 331.0794), suggesting eight degrees of unsaturation. The IR absorption spectrum suggested the presence of phenyl (2947 and 1451 cm^{-1}) and hydroxyl (3378 cm^{-1}) groups. The ^1H and ^{13}C NMR spectra (Table 1) were very similar to those of peapolyphenol C (**8**) (Evidente et al., 2010), indicating that both **1** and **8** shared the same carbon framework. A minor difference between the two compounds was in the substitution patterns of the two aromatic rings in **1**, which were identified as 2,4-dihydroxylated and 3,4-dihydroxylated aromatic rings by analysis of the ^1H–^1H COSY, HMQC, and HMBC spectra (Fig. 2). The ^1H and ^{13}C NMR spectra also showed signals typical of a 1,2,3-propanetriol unit. In fact, the double doublet (J = 9.5 and 3.5 Hz), resonating at δ_H 3.89 and assigned to H-8, showed correlations with two doublets (J = 9.5 Hz at δ_H 4.87 and J = 3.5 Hz at δ_H 4.57) in the COSY system, which were attributed to H-7 and H-9 of the 1,2,3-propanetriol chain (Fig. 2). The correlations observed in the HMQC spectrum supported assignment of the signals at δ_C 76.8 (C-7), 70.9 (C-8), and 66.4 (C-9) of the propanetriol chain. The chemical shift of C-9 at δ_C 66.4 showed an upfield shift, compared to those of other methine carbons at C-7 and C-8, which is caused by the γ-effect due to the C-2′ and C-7 substituents of the hydroxyl group. The gross structure of **1** was established by HMBC correlations of H-7/C-2, C-6, C-9; H-8/C-1, C-1′; and H-9/C-2′, C-6′ (Fig. 2).

The absolute configuration of **1** was determined by chemical methods and by CD data analysis. The configuration of bioactive natural products provides essential information for total synthesis and the molecular mode of action. Thus, characterization of the configuration by X-ray analysis, synthetic methods, or spectroscopic techniques has been important. Unfortunately, this polyphenol **1**, obtained as a gum in very small amounts, is resistant to crystallization, and it is laborious to synthesize totally and apply Mosher's method for the determination of its absolute configuration because of the number of chiral centers in **1**. Thus, compound **1** was converted to flavanol (**1a**) using a Mitsunobu cyclization (Scheme 1) (Krohn et al., 2009; Jew et al., 2000). Compound **1a** was identified as (−)-3′,4′,7-trihydroxyflavan-2,3-*cis*-3,4-*trans*-diol

Table 1
^1H (500 MHz) and ^{13}C NMR (125 MHz) spectroscopic data of rhusopolyphenols A–C (**1**–**3**) in CD_3OD (δ in ppm, J values in parentheses).[a]

No	Rhusopolyphenol A (**1**)		Rhusopolyphenol B (**2**)		Rhusopolyphenol C (**3**)	
	δ_H (J in Hz)	δ_C	δ_H (J in Hz)	δ_C	δ_H (J in Hz)	δ_C
1		130.6		129.9		129.7
2	6.88 d (2.0)	114.6	7.28 dd (8.5, 2.0)	128.7	6.93 d (1.5)	114.5
3		145.0	6.82 dd (8.5, 2.0)	114.6		144.8
4		145.2		157.1		145.2
5	6.77 br s	114.7	6.82 dd (8.5, 2.0)	114.6	6.79 br s	114.5
6	6.77 br s	119.4	7.28 dd (8.5, 2.0)	128.7	6.79 br s	119.5
7	4.87 d (9.5)	76.8	5.01 d (10.0)	76.8	4.60 d (10.0)	81.3
8	3.89 dd (9.5, 3.5)	70.9	3.98 dd (10.0, 3.0)	70.2	3.73 dd (10.0, 8.0)	73.4
9	4.57 d (3.5)	66.4	4.20 d (3.0)	76.2	4.65 d (8.0)	71.5
1′		114.8		111.7		116.1
2′		155.4		155.2		155.0
3′	6.26 d (2.0)	102.1	6.29 d (2.0)	102.2	6.22 d (2.5)	101.7
4′		158.7		159.0		157.6
5′	6.38 dd (8.5, 2.0)	108.5	6.40 dd (8.5, 2.0)	107.4	6.44 dd (8.5, 2.5)	108.5
6′	7.12 d (8.5)	131.3	7.10 d (8.5)	131.3	7.28 d (8.5)	128.2
OMe			3.47 s	55.6		

[a] The assignments were based on ^1H–^1H-COSY, HMQC and HMBC experiments.

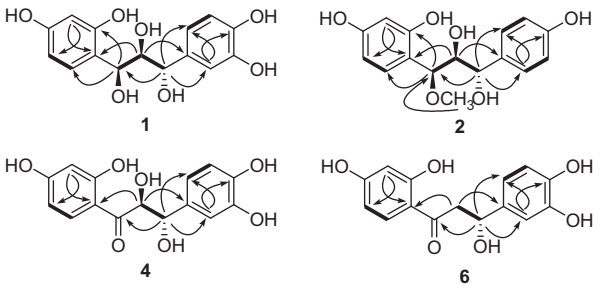

Fig. 2. Key ^{1}H–^{1}H COSY (—) and HMBC (→) correlations of **1**, **2**, **4**, and **6**.

by its ^{1}H NMR, specific rotation, and MS data. Standard S_N2-type Mitsunobu reaction conditions were employed to obtain the enantioselective flavonol which was confirmed to be the expected 2,3-*cis*-3,4-*trans*-configuration in the ^{1}H NMR spectrum of **1a** (Krohn et al., 2009). Remarkably, the theoretically possible formation of a five-membered ring was not observed during the conditions used (Krohn et al., 2009). The CD spectrum of **1a** ($[\theta]_{240}$ −11,500, $[\theta]_{285}$ −17,800) established the absolute configuration to be 2*R*,3*R*,4*S*, as shown in Scheme 1 (Ferreira et al., 2004). Thus, the absolute configuration of **1** was assigned 7*S*,8*S*,9*S* based on the absolute configuration of **1a** because a change in the configuration at C-2 and C-3 in **1a** occurs during the S_N2-type Mitsunobu reaction (Krohn et al., 2009; Jew et al., 2000). On the basis of these considerations, compound **1** was established as shown in Fig. 1, for which the trivial name rhusopolyphenol A is proposed. In addition, the absolute configuration of peapolyphenol C (**8**) was determined to be identical to **1** by comparing the ^{1}H and ^{13}C NMR spectroscopic data, the coupling constants, and its CD spectrum ($[\theta]_{239}$ −19,500, $[\theta]_{281}$ −17,400) with those of **1** ($[\theta]_{236}$ −15,200, $[\theta]_{274}$ −31,300), which is reported for the first time here.

Compound **2** was isolated as a colorless gum. The molecular formula was $C_{16}H_{18}O_6$ based on HR-ESIMS (*m/z* 329.1003 $[M+Na]^+$, calcd. for $C_{16}H_{18}NaO_6$, 329.1001), suggesting eight degrees of unsaturation. Similar to compound **1**, compound **2** showed IR absorptions typical of phenyl and hydroxyl groups. The ^{1}H and ^{13}C NMR spectra (Table 1) were similar to those of **1**, indicating that both **1** and **2** shared the same carbon framework with a 1,2,3-propanetriol unit. The major differences were the presence of a methoxyl group (δ_H 3.47) and different aromatic substitution patterns in **2**, which were identified as 2,4-dihydroxylated and 4-hydroxylated aromatic rings by analysis of the ^{1}H–^{1}H COSY, HMQC, and HMBC spectra (Fig. 2). The location of the methoxyl group was deduced by a downfield shift of C-9 in the ^{13}C NMR spectrum of **2** compared to that of **1** and confirmed by the HMBC correlation from OMe (δ_H 3.47) to C-9 (δ_C 76.2) (Fig. 2). Full assignments of the ^{1}H and ^{13}C NMR spectra (Table 1) were carried out by analysis of the COSY, HMQC, and HMBC data. The absolute configuration of **2** was the same as that of **1** by comparing its coupling constants, specific rotation, and CD data ($[\theta]_{237}$ −25,600, $[\theta]_{283}$ −27,700) with those of **1** ($[\theta]_{236}$ −15,200, $[\theta]_{274}$ −31,300). Thus, compound **2** was determined as shown in Fig. 1, named rhusopolyphenol B.

Compound **3** was obtained as a colorless gum. Its HR-ESIMS data showed an ion peak at *m/z* 331.0790 $[M+Na]^+$ (calcd. for $C_{15}H_{16}NaO_7$, 331.0794) for the molecular formula $C_{15}H_{16}O_7$ with eight degrees of unsaturation. The ^{1}H and ^{13}C NMR spectra (Table 1) were remarkably similar to those of **1**, suggesting that both **1** and **3** belonged to the same carbon framework with a 1,2,3-propanetriol unit. The only differences between them were the chemical shifts and splitting patterns of C-7 [δ_H 4.60 (d, *J* = 10.0 Hz); δ_C

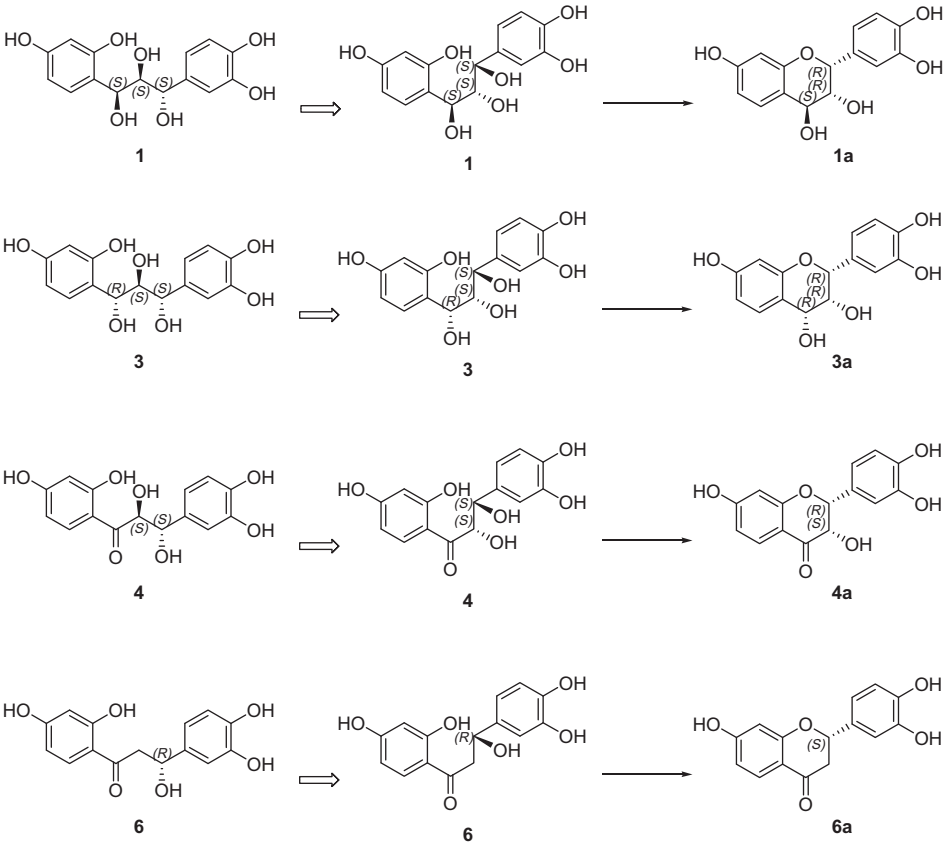

Scheme 1. Reagents and conditions: DEAD, Ph_3P, THF, 3 h.

Table 2
^{1}H (500 MHz) and ^{13}C NMR (125 MHz) spectroscopic data of rhusopolyphenols D–F (**4**–**6**) in CD_3OD (δ in ppm, *J* values in parentheses).[a]

No	Rhusopolyphenol D (**4**)		Rhusopolyphenol E (**5**)		Rhusopolyphenol F (**6**)	
	δ_H (*J* in Hz)	δ_C	δ_H (*J* in Hz)	δ_C	δ_H (*J* in Hz)	δ_C
1		128.7		128.1		128.9
2	7.00 d (2.0)	114.5	7.35 dd (8.5, 2.0)	128.9	6.56 d (2.0)	114.6
3		144.9	6.82 dd (8.5, 2.0)	114.7		145.2
4		145.6		157.7		146.0
5	6.82 d (8.0)	114.6	6.82 dd (8.5, 2.0)	114.7	6.74 d (8.0)	115.2
6	6.88 dd (8.0, 2.0)	119.5	7.35 dd (8.5, 2.0)	128.9	6.41 dd (8.0, 2.0)	119.1
7	4.95 d (11.5)	84.2	4.99 d (12.0)	84.0	5.79 dd (13.0, 1.0)	84.6
8	4.50 d (11.5)	73.1	4.51 d (12.0)	73.1	2.66 dd (14.0, 1.0)3.33 overlapped	51.3
9		193.0		193.1		192.5
1′		112.0		112.0		113.9
2′		163.6		163.7		163.8
3′	6.35 d (2.0)	102.3	6.32 d (2.0)	102.3	6.26 d (2.0)	102.4
4′		165.4		165.4		165.4
5′	6.54 dd (8.5, 2.0)	110.7	6.52 dd (8.5, 2.0)	110.7	6.48 dd (8.5, 2.0)	110.5
6′	7.73 d (8.5)	128.7	7.72 d (8.5)	128.6	7.66 d (8.5)	128.8

[a] The assignments were based on ^{1}H-^{1}H-COSY, HMQC and HMBC experiments.

81.3], C-8 [δ_H 3.73 (dd, *J* = 10.0, 8.0 Hz); δ_C 73.4], and C-9 [δ_H 4.65 (d, *J* = 8.0 Hz); δ_C 71.5] in **3** compared to those of corresponding carbons in **1**, suggesting that they had different configurations at the 1,2,3-propanetriol unit. Similarly, as described for **1**, the absolute configuration of **3** was determined using Mitsunobu cyclization (Scheme 1) (Krohn et al., 2009; Jew et al., 2000), which afforded (−)-3′,4′,7-trihydroxyflavan-2,3-*cis*-3,4-*cis*-diol (**3a**). This was identified by its ^{1}H NMR, specific rotation, and MS data, and its absolute configuration was assigned as 2*R*,3*R*,4*R* by means of the CD data of **3a** ($[\theta]_{242}$ −48,500, $[\theta]_{286}$ −34,800) (Ferreira et al., 2004). Thus, the absolute configuration of **3** was elucidated to be 7*S*,8*S*,9*R*, as described for **1**. On the basis of the evidence, the structure of compound **3** was assigned as shown in Fig. 1, named rhusopolyphenol C.

Compound **4** was isolated as a colorless gum. The molecular formula was $C_{15}H_{14}O_7$ with nine degrees of unsaturation by analysis of the molecular ion peak at *m/z* 329.0645 $[M+Na]^+$ (calcd. for $C_{15}H_{14}NaO_7$, 329.0637) in the HR-ESIMS in combination with ^{1}H and ^{13}C NMR spectra. The IR absorption implied the presence of carbonyl (1713 cm^{-1}), phenyl (2947 and 1451 cm^{-1}), and hydroxyl (3382 cm^{-1}) groups. The ^{1}H and ^{13}C NMR spectra (Table 2) were very similar to those of cilicione-b (**9**) (Ahmed and Al-Howiriny, 2007), suggesting that compound **4** belonged to the same chalcone derivative as **9**. The only difference was the substitution pattern of the aromatic ring in **4**, which was confirmed by analyzing the ^{1}H–^{1}H COSY, HMQC, and HMBC spectra (Fig. 2). The gross structure of **4** was elucidated by analyzing the 2D NMR spectra (COSY, HMQC, and HMBC). The trend for larger couplings in *anti*-orientated protons (*J* = 8–9 Hz) compared to their *syn*-isomers (*J* = 2–3 Hz) has been well established in closely related acyclic polyol derivatives (Wiesler and Nakanishi, 1990), which allowed us to demonstrate that the relative configuration of **4** was the 7,8-*erythro* form. Next, as described for **1**, compound **4** was cyclizated by Mitsunobu reaction to afford compound **4a** for determining its absolute configuration (Scheme 1) (Krohn et al., 2009; Jew et al., 2000). Compound **4a** was identified as (−)-fustin by its ^{1}H NMR, specific rotation, and MS data, and the absolute configuration was established as 2*R*,3*S* by the CD data ($[\theta]_{307}$ −14,600, $[\theta]_{340}$ +8500) (Van Rensburg et al., 1997). Similar to **1**, the absolute configuration of **4** was 7*S*,8*S* based on the absolute configuration of **4a**. Thus, the structure of compound **4** was elucidated as shown in Fig. 1, named rhusopolyphenol D. Additionally, the absolute configuration of cilicione-b (**9**) was identical to **4** by comparing its ^{1}H and ^{13}C NMR spectroscopic data, the coupling constants, and the CD data ($[\theta]_{245}$ +12,600, $[\theta]_{276}$ +17,100, $[\theta]_{290}$ +13,700) with those of **4** ($[\theta]_{246}$ +16,500, $[\theta]_{276}$ +14,300, $[\theta]_{290}$ +12,800), which is suggested for the first time in this study.

The HR-ESIMS data (*m/z* 313.0690 $[M+Na]^+$, calcd. for $C_{15}H_{14}NaO_6$, 313.0688) of **5** indicated that this molecule possessed the molecular formula $C_{15}H_{14}O_6$ with nine degrees of unsaturation. The ^{1}H and ^{13}C NMR spectroscopic data (Table 2) showed high similarity to those of **4**, except for the different substitution pattern of the aromatic ring in **5**, which was determined by analyzing the ^{1}H–^{1}H COSY, HMQC, HMBC spectra. The remaining structural features of **5** were confirmed based on comprehensive 2D NMR studies (COSY, HMQC, and HMBC spectra). The absolute configuration of **5** was the same as that of **4** by comparing its coupling constants, specific rotation, and CD data ($[\theta]_{246}$ +10,600, $[\theta]_{275}$ +15,900, $[\theta]_{291}$ +18,200) with those of **4** ($[\theta]_{246}$ +16,500, $[\theta]_{276}$ +14,300, $[\theta]_{290}$ +12,800). Consequently, compound **5** was established as shown in Fig. 1, named rhusopolyphenol E.

Compound **6** was isolated as a colorless gum. The HR-ESIMS of **6** displayed a molecular ion peak $[M+Na]^+$ at *m/z* 313.0693 (calcd. for $C_{15}H_{14}NaO_6$, 313.0688), consistent with the molecular formula of $C_{15}H_{14}O_6$ with nine of unsaturation. The IR spectrum exhibited absorptions of carbonyl (1705 cm^{-1}), phenyl (2945 and 1499 cm^{-1}), and hydroxyl (3398 cm^{-1}) groups. Inspection of the ^{1}H and ^{13}C NMR spectroscopic data (Table 2) established high similarity to those of (α*R*)-α,3,4,2′,4′-pentahydroxydihydrochalcone (**10**) (Alvarez and Delgado, 1999), except for the chemical shifts of C-7 [δ_H 5.79 (dd, *J* = 13.0, 1.0 Hz); δ_C 84.6] and C-8 [δ_H 2.66 (dd, *J* = 14.0, 1.0 Hz), 3.33 (overlapped); δ_C 51.3] in **6** compared to those [δ_H 2.70 (1H, dd, *J* = 16.5, 3.0 Hz, H-7a), 2.99 (1H, dd, *J* = 16.5, 13.0 Hz, H-7b); δ_C 43.8 (C-7) and δ_H 5.30 (1H, dd, *J* = 13.0, 3.0 Hz, H-8); δ_C 79.8 (C-8)] of corresponding parts in **10**. The differences were confirmed by analyzing the ^{1}H–^{1}H COSY and HMQC spectra, and the HMBC correlations of H-7/C-2, C-6, C-9 and H-8/C-1, C-1′ allowed us to assign an aliphatic carbinol at C-7, a methylene at C-8, and a ketone at C-9 (Fig. 2). The gross structure of **6** was unambiguously established by analyzing the 2D NMR data (COSY, HMQC, and HMBC). Compound **6** was cyclizated using a Mitsunobu reaction to identify its absolute configuration (Scheme 1) (Krohn et al., 2009; Jew et al., 2000). (−)-Butin (**6a**) was synthesized in the reaction, which was identified by its ^{1}H NMR, specific rotation, MS, and CD data ($[\theta]_{292}$ −15,200) (Chokchaisiri et al., 2009). Thus, the absolute configuration of **6** was 7*R* based on the absolute configuration of the synthetic compound, (−)-butin. On the basis of the evidence, the structure of compound **6** was determined as shown in Fig. 1, named rhusopolyphenol F.

Table 3
Cytotoxicity of compounds **4**–**6**, **9**, and **10** against four cultured human cancer cell lines in the SRB bioassay.

Compound	IC_{50} (μM)[a]			
	A549	SK-OV-3	SK-MEL-2	HCT-15
4	17.05 ± 1.21[b]	17.41 ± 1.71	13.18 ± 1.19	8.54 ± 0.83
5	16.42 ± 0.31	12.10 ± 0.90	4.38 ± 0.49	12.91 ± 1.43
6	18.51 ± 1.80	10.32 ± 0.97	9.74 ± 0.13	11.65 ± 2.66
9	18.57 ± 1.40	12.38 ± 1.54	10.13 ± 1.25	17.82 ± 3.23
10	3.31 ± 0.68	4.28 ± 0.13	7.70 ± 1.18	8.81 ± 0.79
Doxorubicin[c]	0.016 ± 0.005	0.027 ± 0.003	0.036 ± 0.001	1.073 ± 0.067

[a] 50% inhibitory concentration; the concentration of compound that caused a 50% inhibition in cell growth.
[b] Data are expressed as mean ± SEM of three independent experiments.
[c] Doxorubicin as a positive control.

Compound **7**, (2*R*,3*S*,10*S*)-7,8,9,13-tetrahydroxy-2-(3,4-dihydroxyphenyl)-2,3-*trans*-3,4-*cis*-2,3,10-trihydrobenzopyrano[3,4-*c*]-2-benzopyran-1-one was previously isolated from the heartwood of *Peltophorum africanum* (Bam et al., 1990). But, its ^{13}C NMR spectroscopic data has not been reported, though that of its hexamethyl ether was published (Bam et al., 1990). Full NMR data assignments of **7** were thus performed by analyzing the 2D NMR data (including DEPT, HMQC, HMBC, and NOESY). The absolute configuration was identified by coupling constants ($J_{2,3}$ = 2.5 Hz, $J_{3,4}$ = 3.0 Hz) and its CD spectrum showing the positive Cotton effect in the 225–240 nm consistent with those of the reported corresponding compounds (Bam et al., 1990). To the best of our knowledge, the ^{13}C NMR spectroscopic data is reported in this study for the first time.

The other known compounds were identified as peapolyphenol C (**8**) (Evidente et al., 2010), cilicione-b (**9**) (Ahmed and Al-howiriny, 2007), and (α*R*)-α,3,4,2′,4′-pentahydroxydihydrochalcone (**10**) (Alvarez and Delgado, 1999) by comparing their spectroscopic data with values reported previously. These known compounds **7**–**10** were isolated from this plant for the first time.

The fermentation or hot water extraction might change some constitutions and structures of naturally occurring compounds. In order to identify whether the isolated compounds **1**–**10** were genuine natural compounds or artifacts, *R. verniciflua* barks were extracted with 50% EtOH and 80% MeOH in H_2O at room temperature to obtain crude EtOH and MeOH extracts, respectively. HPLC analyses of the extracts indicated that the chemical profiles are quite similar to each other. The peaks of all compounds except for **9** were observed in the HPLC chromatogram of the EtOH extract, which was also confirmed by LC-MS analyses. The peak corresponding to **9** could be identified in the HPLC chromatogram of the MeOH extract. This evidence proves that the compounds **1**–**10** are genuine natural products.

To evaluate the isolated compounds **1**–**10** as cytotoxic agents, evaluation of their antiproliferative activities was performed against the A549, SK-OV-3, SK-MEL-2, and HCT-15 cell lines using the SRB bioassay (Skehan et al., 1990). Compounds **4**–**6**, **9**, and **10** showed antiproliferative activity against the tested cells with IC_{50} values of 3.31–18.51 μM, but the other compounds were inactive (IC_{50} > 30.0 μM) (Table 3). Compound **10** exhibited the most potent antiproliferative activity against A549, SK-OV-3, SK-MEL-2, and HCT-15 cells, with IC_{50} values of 3.31, 4.28, 7.70, and 8.81 μM, respectively. Although more structurally related compounds need to be tested to confirm this hypothesis, it appears that the presence of a ketone group at C-9 in these molecules is essential for manifesting the activity in such polyphenols as compounds **4**–**6**, **9**, and **10** showed the inhibitory activity against cell proliferation in the tested lines, whereas the other compounds **1**–**3**, **7**, and **8** were inactive. The lipophilicity may modulate the in vitro cytotoxicity of compounds **1**–**10**. Compounds **4**–**6**, **9**, and **10**, which were more lipophilic than inactive compounds **1**–**3**, **7**, and **8** (estimated on the basis of HPLC retention time and TLC Rf value), showed higher cytotoxicities (Table 3). This result is in agreement with other reports of increases in cytotoxicity with the absence or with the decreasing number of hydroxyl groups (Bao et al., 2005; Sun et al., 2003). Higher lipophilicity may lead to facilitated penetration through the lipophilic plasma membrane of the tumor cells, and subsequently, to higher cytotoxicity (Beekman et al., 1997). The change in the hydroxyl group position present in the active compounds, leads to important changes in cytotoxicity. Compound **4**, without a hydroxyl group at C-6′, was twice as potent against the HCT-15 cell line with respect to that of **9**, and compound **5**, without a hydroxyl group at C-3, was three times more potent compared to **4** against the SK-MEL-2 cell line. In particular, the change in hydroxyl group location at positions C-7 and C-8 affected the significant changes in the cytotoxicity of **6** and **10**, and the presence of a hydroxyl group at C-8 in **10** led to an increase in activity against all the tested cell lines in comparison to that of **6**. The change in the hydroxyl group position in molecules results in alteration of the reactive position which may be associated with the pro-oxidant effect influencing inhibition of cell viability, induction of apoptosis and necrosis, and cell cycle arrest in cancer cells through electron transfer reactions leading to moderate formation of ROS (Sanchez-Tena et al., 2012). The alteration of pro-oxidant effect may cause different potency in cytotoxicity of the active compounds.

Inflammatory gene expression is often negatively correlated with cancer stage and prognosis (Chang et al., 2004; Galon et al., 2006; Wang et al., 2006). Moreover, non-steroidal anti-inflammatory drugs show preventive effects against cancer (Ulrich et al., 2006). Therefore, cancer and inflammation are related by epidemiology, histopathology, and inflammatory profiles (Rakoff-Nahoum, 2006). As inflammation plays a crucial role in tumor progression (Coussens and Werb, 2002), the anti-inflammatory activities of polyphenols **1**–**10** isolated from *R. verniciflua* in lipopolysaccharide (LPS)-activated BV-2 cells were evaluated by measuring the nitric oxide (NO) levels produced. BV-2 has both the phenotypic and functional properties of reactive microglia cells (Blasi et al., 1990) and is activated following stimulation by various agents such as

Table 4
Inhibitory effect of compounds **1**–**10** on nitric oxide (NO) production in LPS-activated BV-2 cells.

Compound	IC_{50} (μM)[a]	Cell viability (%)[b]	Compound	IC_{50} (μM)[a]	Cell viability (%)[b]
1	91.02	94.1 ± 3.5*	7	>500	104.3 ± 3.1
2	31.29	100.0 ± 5.1	8	75.24	96.8 ± 6.9
3	52.40	92.8 ± 2.8*	9	74.51	96.7 ± 2.6
4	42.51	97.4 ± 4.2	10	12.70	96.8 ± 4.2
5	28.90	102.5 ± 5.3	NMMA[c]	18.29	101.3 ± 4.5
6	84.05	90.5 ± 4.9*			

Results are averages of three independent experiments, and data are expressed as mean ± SD (*p-value < 0.05).
[a] IC_{50} value of each compound was defined as the concentration (μM) that caused 50% inhibition of NO production in LPS-activated BV-2 cells.
[b] Cell viability after treatment with 20 μM of each compound is expressed as a percentage (%) of the LPS only treatment group.
[c] NMMA was the positive control.

LPS (Dheen et al., 2007). Activated BV-2 cells exhibit various inflammatory responses including production of the proinflammatory factor NO (Hanisch, 2002). It has been known that polyphenols exhibit anti-inflammatory properties (Muldoon and Kritchevsky, 1996). In this study, compounds **5** and **10** significantly inhibited NO levels (IC_{50} values < 30 μM) in LPS-stimulated BV-2 without cell toxicity (Table 4). In particular, compound **10** exhibited the highest inhibitory activity with an IC_{50} of 12.70 μM, which was more potent than that of N^G-monomethyl-L-arginine (L-NMMA), an inducible NO synthase inhibitor (Reif and McCreedy, 1995). Interestingly, the presence of a ketone group at C-9 in these polyphenols played an important role in the anti-inflammatory properties as well as cytotoxic activity.

3. Concluding remarks

This study dealt with the isolation and biological activity of 10 polyphenols including the structural elucidation of six new polyphenols, rhusopolyphenols A–F (**1**–**6**) from *R. verniciflua* bark through bioactivity-guided isolation techniques. It was confirmed that the polyphenols represented a portion of the molecules with cytotoxic and anti-inflammatory activities. Although all compounds were not active, compounds **4**–**6**, **9**, and **10** can be considered highly cytotoxic agents (IC_{50} values < 20 μM) in A549, SK-OV-3, SK-MEL-2, and HCT-15 cell lines, whereas compounds **5** and **10** exhibited an anti-inflammatory effect by inhibiting NO levels (IC_{50} values < 30 μM) in LPS-stimulated BV-2 cells. Taking into account that compounds **5** and **10** showed higher antitumor and anti-inflammatory activities, it is suggested that they might be useful as bioactive molecules for regulating various cancers and inflammation-related diseases and their structures can be considered as new lead molecules for the design of analogs with therapeutic potential. These results also demonstrate that the use of *R. verniciflua* as Korean traditional medicine to treat inflammatory diseases and various cancers is reasonable, because the polyphenols were isolated with cytotoxic and anti-inflammatory effects as a main component.

4. Experimental

4.1. General experimental procedures

Optical rotations were measured on a Jasco P-1020 polarimeter (Jasco, Easton, MD, USA). IR spectra were recorded on a Bruker IFS-66/S FT-IR spectrometer (Bruker, Karlsruhe, Germany). Circular dichroism (CD) spectra were measured on a Jasco J-715 spectropolarimeter (Jasco, Easton, MD, USA). Ultraviolet (UV) spectra were recorded with a Shimadzu UV-1601 UV–Visible spectrophotometer (Shimadzu, Tokyo, Japan). Electron spray ionization (ESI) and high-resolution (HR)-ESI mass spectra were acquired on a SI-2/LCQ DecaXP Liquid chromatography (LC)-mass spectrometer (Thermo Scientific, West Palm Beach, PL, USA). Nuclear magnetic resonance (NMR) spectra were obtained using a Varian UNITY INOVA 500 NMR spectrometer (Varian, Palo Alto, CA, USA) operating at 500 MHz (^{1}H) and 125 MHz (^{13}C), with chemical shifts given in ppm (δ). Preparative high performance liquid chromatography (HPLC) used a Gilson 306 pump (Gilson, Middleton, WI, USA) with a Shodex refractive index detector (Shodex, New York, NY, USA). Column chromatography (CC) was performed with silica gel 60 (Merck, 70–230 mesh and 230–400 mesh) and RP-C_{18} silica gel (Merck, 230–400 mesh). The packing material for molecular sieve CC was Sephadex LH-20 (Pharmacia, Uppsala, Sweden). Merck precoated silica gel F_{254} plates and reversed-phase (RP)-18 F_{254s} plates (Merck, Darmstadt, Germany) were used for thin-layer chromatography (TLC). Spots were detected on TLC under UV light or by heating after spraying with anisaldehyde-sulfuric acid.

4.2. Plant material

R. verniciflua bark was collected in Hoengseong, Gangwon-do, Korea, in March 2010. The plant material was identified by one of the authors (K.R. Lee). A voucher specimen (SKKU-RV 2010-3) was deposited at the Farm Corporation, Dongyi's Farms, Boryung, Chungcheongnam-do, Korea.

4.3. Extraction and isolation

Air-dried and pulverized plant material (1.3 kg) was soaked in distilled H_2O (10 L), thus begin heated until reflux began and held for 1 h with the material in boiling water then being cooled. The material in the cooled water was then fermented at 30 °C for 35 h to augment the active constituents and remove toxic components by *A. oryzae*. The fermented material was extracted with H_2O twice (each 20 L × 3 h) under conditions of reflux and the whole filtered. The filtrate was evaporated in vacuo to obtain a crude extract (120 g), which was further extracted with EtOH to afford a crude EtOH extract (60 g). The EtOH extract (10 g) was subjected to C_{18} reverse-phased silica gel CC, eluted with a gradient of MeOH–H_2O (2:3 → 1:0) to yield six fractions (fractions A–F). Each fraction was evaluated for cytotoxic activity against A549, SK-OV-3, SK-MEL-2, and HCT-15 human tumor cell lines using the SRB bioassay, and a bioactivity-guided fractionation method was used for the isolation work. Fractions B and C showed weak cytotoxicity, whereas fractions D and E exhibited significant cytotoxicity against the tested cell lines. The active fraction B (3.5 g) was applied to Sephadex LH-20 and eluted with MeOH–H_2O (4:1) to give five subfractions (B1–B5). Fraction B5 (450 mg) was further purified by semi-preparative HPLC using a solvent system of MeOH–H_2O (2:3) at a flow rate of 2.0 mL/min (Econosil RP-18 column; 250 × 10 mm; 10 μm particle size; Shodex refractive index detector) to afford **7** (4 mg). The active fraction C (550 mg) was subjected to Sephadex LH-20 chromatography, eluted with MeOH–H_2O (4:1) to yield five subfractions (C1–C5). Fraction C4 (130 mg) was purified by semi-preparative HPLC, as described above, using a solvent system of MeOH–H_2O (9:11) to provide **9** (15 mg). The active fraction D (560 mg) was applied to a silica gel column eluted with $CHCl_3$–MeOH (17:1) to give six subfractions (D1–D6). Fraction D3 (185 mg) was purified by semi-preparative HPLC, as described above, using a solvent system of MeOH–H_2O (9:11) to obtain compounds **2** (5 mg), **5** (10 mg), and **8** (7 mg). Fraction D4 (50 mg) was purified by semi-preparative HPLC, as described above, using a solvent system of MeOH–H_2O (1:1) to afford **10** (18 mg). Finally, active fraction E (1.9 g) was subjected to silica gel CC eluted with $CHCl_3$–MeOH (15:1) to furnish five subfractions (E1–E5). Fraction E3 (350 mg) was purified by semi-preparative HPLC, using a solvent system of MeOH–H_2O (3:2) to give **4** (4 mg). Fraction E5 (800 mg) was subjected to C_{18} reverse-phased silica gel CC and eluted with MeOH–H_2O (2:3 → 4:1, gradient system) to yield two subfractions (E51 and E52). Fraction E51 (150 mg) was purified by semi-preparative HPLC, using a solvent system of MeOH–H_2O (3:7) to obtain compounds **1** (4 mg) and **3** (3 mg). Fraction E52 (110 mg) was purified by semi-preparative HPLC, using a solvent system of MeOH–H_2O (3:2) to yield **6** (5 mg).

4.3.1. Rhusopolyphenol A (*1*)

Ccolorless gum; $[\alpha]_D^{25}$ −23.8 (*c* 0.18, MeOH); UV (MeOH) λ_{max} nm (log ε): 218 (3.9), 275 (2.6); CD (MeOH): $[\theta]_{236}$ −15,200, $[\theta]_{274}$ −31,300; IR (KBr) ν_{max} cm^{-1}: 3378, 2947, 2834, 2503, 1661, 1451, 1120, 1030; for ^{1}H (500 MHz) and ^{13}C (125 MHz) NMR spectroscopic data, see Table 1; ESIMS (positive-ion mode) *m/z* 331

$[M+Na]^+$; HR-ESIMS (positive-ion mode) *m/z* 331.0797 $[M+Na]^+$ (calcd. for $C_{15}H_{16}NaO_7$, 331.0794).

4.3.2. Rhusopolyphenol B (**2**)

Colorless gum; $[\alpha]_D^{25}$ −19.1 (*c* 0.20, MeOH); UV (MeOH) λ_{max} nm (log ε): 218 (3.9), 275 (2.5); CD (MeOH): $[\theta]_{237}$ −25,600, $[\theta]_{283}$ −27,700; IR (KBr) ν_{max} cm^{-1}: 3383, 2948, 2836, 2504, 1661, 1452, 1120, 1031; for ^1H (500 MHz) and ^{13}C (125 MHz) NMR spectroscopic data, see Table 1; ESIMS (positive-ion mode) *m/z* 329 $[M+Na]^+$; HR-ESIMS (positive-ion mode) *m/z* 329.1003 $[M+Na]^+$ (calcd. for $C_{16}H_{18}NaO_6$, 329.1001).

4.3.3. Rhusopolyphenol C (**3**)

Colorless gum; $[\alpha]_D^{25}$ +34.2 (*c* 0.13, MeOH); UV (MeOH) λ_{max} nm (log ε): 218 (3.9), 275 (2.6); CD (MeOH): $[\theta]_{250}$ −11,200, $[\theta]_{291}$ +2500; IR (KBr) ν_{max} cm^{-1}: 3419, 2947, 2835, 2506, 1644, 1449, 1058, 1033; for ^1H (500 MHz) and ^{13}C (125 MHz) NMR spectroscopic data, see Table 1; ESIMS (positive-ion mode) *m/z* 331 $[M+Na]^+$; HR-ESIMS (positive-ion mode) *m/z* 331.0790 $[M+Na]^+$ (calcd. for $C_{15}H_{16}NaO_7$, 331.0794).

4.3.4. Rhusopolyphenol D (**4**)

Colorless gum; $[\alpha]_D^{25}$ +12.7 (*c* 0.20, MeOH); UV (MeOH) λ_{max} nm (log ε): 213 (4.1), 285 (3.2); CD (MeOH): $[\theta]_{246}$ +16,500, $[\theta]_{276}$ +14,300, $[\theta]_{290}$ +12,800; IR (KBr) ν_{max} cm^{-1}: 3382, 2947, 2836, 2502, 1713, 1451, 1120, 1030; for ^1H (500 MHz) and ^{13}C (125 MHz) NMR spectroscopic data, see Table 2; ESIMS (positive-ion mode) *m/z* 329 $[M+Na]^+$; HR-ESIMS (positive-ion mode) *m/z* 329.0645 $[M+Na]^+$ (calcd. for $C_{15}H_{14}NaO_7$, 329.0637).

4.3.5. Rhusopolyphenol E (**5**)

Colorless gum; $[\alpha]_D^{25}$ +10.8 (*c* 0.45, MeOH); UV (MeOH) λ_{max} nm (log ε): 214 (4.1), 286 (3.0); CD (MeOH): $[\theta]_{246}$ +10,600, $[\theta]_{275}$ +15,900, $[\theta]_{291}$ +18,200; IR (KBr) ν_{max} cm^{-1}: 3382, 2947, 2833, 2502, 1712, 1451, 1115, 1031; for ^1H (500 MHz) and ^{13}C (125 MHz) NMR spectroscopic data, see Table 2; ESIMS (positive-ion mode) *m/z* 313 $[M+Na]^+$; HR-ESIMS (positive-ion mode) *m/z* 313.0690 $[M+Na]^+$ (calcd. for $C_{15}H_{14}NaO_6$, 313.0688).

4.3.6. Rhusopolyphenol F (**6**)

Amorphous solid; $[\alpha]_D^{25}$ +19.4 (*c* 0.25, MeOH); UV (MeOH) λ_{max} nm (log ε): 214 (4.1), 284 (3.4), 320 (3.3); CD (MeOH): $[\theta]_{245}$ +6500, $[\theta]_{280}$ +12,100, $[\theta]_{293}$ +8900; IR (KBr) ν_{max} cm^{-1}: 3398, 2945, 2832, 2501, 1705, 1499, 1120, 1030; for ^1H (500 MHz) and ^{13}C (125 MHz) NMR spectroscopic data, see Table 2; ESIMS (positive-ion mode) *m/z* 313 $[M+Na]^+$; HR-ESIMS (positive-ion mode) *m/z* 313.0693 $[M+Na]^+$ (calcd. for $C_{15}H_{14}NaO_6$, 313.0688).

4.3.7. (2R,3S,10S)-7,8,9,13-Tetrahydroxy-2-(3,4-dihydroxyphenyl)-2,3-trans-3,4-cis-2,3,10-trihydrobenzopyrano[3,4-c]-2-benzopyran-1-one (**7**)

Amorphous solid; $[\alpha]_D^{25}$ −47.4 (*c* 0.15, MeOH); UV (MeOH) λ_{max} nm (log ε): 214 (4.0), 276 (3.6); CD (MeOH): $[\theta]_{225}$ +59,500, $[\theta]_{230}$ +65,300, $[\theta]_{270}$ −5200; IR (KBr) ν_{max} cm^{-1}: 3347, 2925, 1712, 1515, 1493, 1210, 1118, 1030; ^1H NMR (500 MHz, CD_3OD): δ 7.07 (1H, s, H-2″), 6.80 (1H, d, *J* = 2.0 Hz, H-2′), 6.79 (1H, d, *J* = 8.5 Hz, H-5′), 6.69 (1H, d, *J* = 8.5 Hz, H-5), 6.67 (1H, dd, *J* = 8.5, 2.0 Hz, H-6′), 6.41 (1H, d, *J* = 2.0 Hz, H-8), 6.27 (1H, dd, *J* = 8.5, 2.0 Hz, H-6), 5.54 (1H, d, *J* = 2.5 Hz, H-2), 4.91 (1H, dd, *J* = 3.0, 2.5 Hz, H-3), 4.05 (1H, d, *J* = 3.0 Hz, H-4); ^{13}C NMR (125 MHz, CD_3OD): δ 166.5 (C-7″), 157.2 (C-7), 153.3 (C-8a), 145.2 (C-3′), 144.8 (C-4′, C-3″), 142.5 (C-5″), 139.8 (C-4″), 130.1 (C-5), 129.5 (C-1′), 121.8 (C-6″), 116.4 (C-6′), 115.2 (C-5′), 113.7 (C-1″), 112.1 (C-2′), 110.8 (C-5a), 108.2 (C-6, C-2″), 101.8 (C-8), 77.2 (C-3), 76.8 (C-2), 26.1 (C-4); HR-ESIMS (positive-ion mode) *m/z* 447.0689 $[M+Na]^+$ (calcd. for $C_{22}H_{16}NaO_9$, 447.0692).

4.4. General procedure for Mitsunobu reaction

To a solution of individual polyphenols **1**, **3**, **4**, and **6** (0.005 mmol) in anhydrous THF (0.05 ml) was added Ph_3P (2 mg, 0.008 mmol). Each mixture was stirred for 15 min, and DEAD (Diethyl azodicarboxylate) (1.5 μl, 0.008 mmol) was added dropwise to the reaction mixture. After stirring for 3 h at room temperature (reaction monitored by TLC), each reaction mixture was diluted with EtOAc (5 ml) and washed with H_2O (5 ml) and brine (4 ml). Each organic phase was then dried ($MgSO_4$), filtered, and concentrated under reduced pressure to produce a brown residue. Each residue was purified with a silica gel Waters Sep-Pak Vac 6 cc (*n*-Hexane–EtOAc, 3:1) (Water, Milford, MA, USA) to give the cyclized products **1a**, **3a**, **4a**, and **6a** as amorphous solids, respectively.

4.4.1. (−)-3′,4′,7-Trihydroxyflavan-2,3-cis-3,4-trans-diol (**1a**)

Amorphous solid; 75% yield; $[\alpha]_D^{25}$ −7.4 (*c* 0.05, MeOH); CD (MeOH): $[\theta]_{240}$ −11,500, $[\theta]_{285}$ −17,800; IR (KBr) ν_{max} cm^{-1}: 3407, 2912, 1585, 1483, 1310, 1241, 1030; ^1H NMR (500 MHz, CD_3OD): δ 6.97 (1H, d, *J* = 2.0 Hz, H-2′), 6.85 (1H, d, *J* = 8.5 Hz, H-5), 6.79 (1H, d, *J* = 8.5, 2.0 Hz, H-6′), 6.75 (1H, dd, *J* = 8.5 Hz, H-5′), 6.45 (1H, d, *J* = 2.0 Hz, H-8), 6.22 (1H, dd, *J* = 8.5, 2.0 Hz, H-6), 5.04 (1H, d, *J* = 2.5 Hz, H-2), 4.56 (1H, d, *J* = 6.0 Hz, H-4), 4.45 (1H, dd, *J* = 6.0, 2.5 Hz, H-3); ESIMS (positive-ion mode) *m/z* 313 $[M+Na]^+$.

4.4.2. (−)-3′,4′,7-Trihydroxyflavan-2,3-cis-3,4-cis-diol (**3a**)

Amorphous solid; 80% yield; $[\alpha]_D^{25}$ −17.3 (*c* 0.05, MeOH); CD (MeOH): $[\theta]_{242}$ −48,500, $[\theta]_{286}$ −34,800; IR (KBr) ν_{max} cm^{-1}: 3427, 2930, 1610, 1501, 1338, 1241, 1030; ^1H NMR (500 MHz, CD_3OD): δ 7.01 (1H, d, *J* = 2.0 Hz, H-2′), 6.88 (1H, d, *J* = 8.0 Hz, H-5), 6.82 (1H, d, *J* = 8.5, 2.0 Hz, H-6′), 6.77 (1H, dd, *J* = 8.5 Hz, H-5′), 6.45 (1H, d, *J* = 2.0 Hz, H-8), 6.21 (1H, dd, *J* = 8.0, 2.0 Hz, H-6), 4.98 (1H, d, *J* = 1.0 Hz, H-2), 4.75 (1H, d, *J* = 4.0 Hz, H-4), 4.24 (1H, dd, *J* = 4.0, 1.0 Hz, H-3); ESIMS (positive-ion mode) *m/z* 313 $[M+Na]^+$.

4.4.3. (−)-Fustin (**4a**)

Amorphous solid; 75% yield; $[\alpha]_D^{25}$ −11.4 (*c* 0.05, MeOH); CD (MeOH): $[\theta]_{307}$ −14,600, $[\theta]_{340}$ +8500; IR (KBr) ν_{max} cm^{-1}: 3415, 2932, 1665, 1500, 1398, 1245, 1030; ^1H NMR (500 MHz, CD_3OD): δ 7.68 (1H, d, *J* = 8.5 Hz, H-5), 6.87 (1H, d, *J* = 2.0 Hz, H-2′), 6.77 (1H, d, *J* = 8.0, 2.0 Hz, H-6′), 6.73 (1H, dd, *J* = 8.0 Hz, H-5′), 6.45 (1H, dd, *J* = 8.5, 2.0 Hz, H-6), 6.30 (1H, d, *J* = 2.0 Hz, H-8), 5.05 (1H, d, *J* = 6.0 Hz, H-2), 4.45 (1H, dd, *J* = 6.0 Hz, H-3); ESIMS (positive-ion mode) *m/z* 311 $[M+Na]^+$.

4.4.4. (−)-Butin (**6a**)

Amorphous solid; 78% yield; $[\alpha]_D^{25}$ −32.6 (*c* 0.05, MeOH); CD (MeOH): $[\theta]_{292}$ −15,200; IR (KBr) ν_{max} cm^{-1}: 3454, 2930, 1662, 1580, 1502, 1361, 1345, 1285, 1170, 1030; ^1H NMR (500 MHz, CD_3OD): δ 7.68 (1H, d, *J* = 8.0 Hz, H-5), 6.85 (1H, d, *J* = 2.0 Hz, H-2′), 6.76 (1H, dd, *J* = 8.0 Hz, H-5′), 6.71 (1H, d, *J* = 8.0, 1.5 Hz, H-6′), 6.42 (1H, dd, *J* = 8.5, 2.0 Hz, H-6), 6.29 (1H, d, *J* = 2.0 Hz, H-8), 5.21 (1H, dd, *J* = 13.0, 3.0 Hz, H-2), 2.91 (1H, dd, *J* = 17.0, 13.0 Hz, H-3a), 2.65 (1H, dd, *J* = 17.0, 3.0 Hz, H-3b); ESIMS (positive-ion mode) *m/z* 295 $[M+Na]^+$.

4.5. Cell cultures

All tumor cell cultures were maintained using RPMI1640 cell growth medium (Gibco, Carlsbad, CA), supplemented with 5% fetal bovine serum (FBS) (Gibco), 100 units/ml penicillin and 100 μg/ml streptomycin. Human tumor cell lines such as A549 (non-small cell lung carcinoma), SK-OV-3 (ovary malignant ascites), SK-MEL-2

(skin melanoma), and HCT-15 (colon adenocarcinoma) were provided by the National Cancer Institute (NCI). BV-2 (microglia from murine) was generously provided by Dr. E. Choi from Korea University (Seoul, Korea). It was maintained in Dulbecco's modified Eagle (DMEM) medium supplemented with 5% FBS, 100 units/ml penicillin and 100 μg/ml streptomycin. All cells were incubated at 37 °C in a humidified incubator with 5% CO_2.

4.6. Cytotoxicity assessment

The cytotoxicity of the compounds against cultured human tumor cell lines was evaluated by SRB method. The assays were performed at the Korea Research Institute of Chemical Technology. Each tumor cell line was inoculated over standard 96-well flat-bottom microplates and then incubated for 24 h at 37 °C in a humidified atmosphere of 5% CO_2. The attached cells were then incubated with the serially diluted samples. After continuous exposure to the compounds for 48 h, the culture medium was removed from each well and the cells were fixed with 10% cold trichloroacetic acid at 4 °C for 1 h. After washing with tap water, the cells were stained with 0.4% SRB dye and incubated for 30 min at room temperature. The cells were washed again and then solubilized with 10 mM unbuffered Tris base solution (pH 10.5). The absorbance was measured spectrophotometrically at 520 nm with a microtiter plate reader. Doxorubicin (Sigma Chemical Co., ⩾98%) was used as the positive control. Doxorubicin had IC_{50} values against A549, SK-OV-3, SK-MEL-2, and HCT-15 of 0.01, 0.02, 0.03, and 1.07 μM, respectively.

4.7. Measurement of NO production and cell viability in LPS-activated BV-2 cells

BV-2 microglia cells were stimulated with 100 ng/mL LPS in the presence or absence of samples for 24 h. Nitrite in the culture media, a soluble oxidation product of NO, was measured by the Griess reaction. The supernatant (50 μl) was harvested and mixed with an equal volume of Griess reagent (1% sulfanilamide, 0.1% *N*-1-napthylethylenediamine dihydrochloride in 5% phosphoric acid). After 10 min, the absorbance at 540 nm was measured using a microplate reader (Emax, Molecular Device, Sunnyvale, CA, USA). Graded sodium nitrite solutions were used as standards to calculate nitrite concentration. Cell viability was measured using a 3-[4,5-dimethylthiazol-2-yl]-2,5-diphenyltetrazolium bromide (MTT) colorimetric assay. N^G-monomethyl-L-arginine (L-NMMA, Sigma, St. Louis, MO, USA), a well-known NO synthase inhibitor, served as a positive control.

Acknowledgments

This work was supported by the Postdoctoral Research Program of Sungkyunkwan University (2012). We thank Drs. E.J. Bang, S.G. Kim, and J.J. Seo at the Korea Basic Science Institute for their aid in the NMR and MS spectra measurements.

Appendix A. Supplementary data

Supplementary data associated with this article can be found, in the online version, at http://dx.doi.org/10.1016/j.phytochem.2013.05.005.

References

Ahmed, B., Al-Howiriny, T.A., 2007. Two new hydroxy chalcone derivatives from *Thymus cilicicus*. Z. Naturforsch. 62b, 121–124.
Alvarez, L., Delgado, G., 1999. *C*- and *O*-Glycosyl-α-hydroxydihydrochalcones from *Eysenhardtia polystachya*. Phytochemistry 50, 681–687.
Bam, M., Malan, J.C.S., Young, D.A., Brandt, E.V., Ferreira, D., 1990. Profisetinidin-type 4-arylflavan-3-ols and related δ-lactones. Phytochemistry 29, 283–287.
Bao, B., Sun, Q., Yao, X., Hong, J., Lee, C.O., Sim, C.J., Im, K.S., Jung, J.H., 2005. Cytotoxic bisindole alkaloids from a marine sponge *Spongosorites* sp. J. Nat. Prod. 68, 711–715.
Beekman, A.C., Woerdenbag, H.J., van Uden, W., Pras, N., Konings, A.W.T., Wikstroem, H.V., Schmidt, T.J., 1997. Structure-cytotoxicity relationships of some helenanolide-type sesquiterpene lactones. J. Nat. Prod. 60, 252–257.
Blasi, E., Barluzzi, R., Bocchini, V., Mazzolla, R., Bistoni, F., 1990. Immortalization of murine microglial cells by a v-raf/v-myc carrying retrovirus. J. Neuroimmunol. 27, 229–237.
Bravo, L., 1998. Polyphenols: chemistry, dietary sources, metabolism, and nutritional significance. Nutr. Rev. 56, 317–333.
Chang, H.Y., Sneddon, J.B., Alizadeh, A.A., Sood, R., West, R.B., Montgomery, K., Chi, J.T., van de Rijn, M., Botstein, D., Brown, P.O., 2004. Gene expression signature of fibroblast serum response predicts human cancer progression: similarities between tumors and wounds. PLoS Biol. 2, E7.
Chokchaisiri, R., Suaisom, C., Sriphota, S., Chindaduang, A., Chuprajob, T., Suksamrarn, A., 2009. Bioactive flavonoids of the flowers of *Butea monosperma*. Chem. Pharm. Bull. 57, 428–432.
Chung, K.T., Wong, T.Y., Wei, C.I., Huang, Y.W., Lin, Y., 1998. Tannins and human health: a review. Crit. Rev. Food. Sci. Nutr. 38, 421–464.
Coates, E.M., Popa, G., Gill, C.I., McCann, M.J., McDougall, G.J., Stewart, D., Rowland, I., 2007. Colon-available raspberry polyphenols exhibit anti-cancer effects on in vitro models of colon cancer. J. Carcinog. 6, 4.
Coussens, L.M., Werb, Z., 2002. Inflammation and cancer. Nature 420, 860–867.
Dai, J., Mumper, R.J., 2010. Plant phenolics: extraction, analysis and their antioxidant and anticancer properties. Molecules 15, 7313–7352.
Dheen, S.T., Kaur, C., Ling, E.A., 2007. Microglial activation and its implications in the brain diseases. Curr. Med. Chem. 14, 1189–1197.
Evidente, A., Cimmino, A., Fernandez-Aparicio, M., Andolfi, A., Rubiales, D., Motta, A., 2010. Polyphenols, including the new peapolyphenols A–C, from pea root exudates stimulate *Orobanche foetida* seed germination. J. Agric. Food Chem. 58, 2902–2907.
Ferreira, D., Marais, J.P.J., Slade, D., Walker, L.A., 2004. Circular dichroic properties of flavan-3,4-diols. J. Nat. Prod. 67, 174–178.
Galon, J., Costes, A., Sanchez-Cabo, F., Kirilovsky, A., Mlecnik, B., Lagorce-Pagès, C., Tosolini, M., Camus, M., Berger, A., Wind, P., Zinzindohoué, F., Bruneval, P., Cugnenc, P.H., Trajanoski, Z., Fridman, W.H., Pagès, F., 2006. Type, density, and location of immune cells within human colorectal tumors predict clinical outcome. Science 313, 1960–1964.
Gerritsen, M.E., Carley, W.W., Ranges, G.E., Shen, C.P., Phan, S.A., Ligon, G.F., Perry, C.A., 1995. Flavonoids inhibit cytokine-induced endothelial cell adhesion protein gene expression. Am. J. Pathol. 147, 278–292.
Hanisch, U.K., 2002. Microglia as a source and target of cytokines. Glia 40, 140–155.
Hour, T.C., Liang, Y.C., Chu, I.S., Lin, J.K., 1999. Inhibition of eleven mutagens by various tea extracts, (−)epigallocatechin-3-gallate, gallic acid and caffeine. Food Chem. Toxicol. 37, 569–579.
Jew, S., Kim, H., Bae, S., Kim, J., Park, H., 2000. Enantioselective synthetic method for 3-hydroxyflavanones: an approach to (2*R*,3*R*)-3′,4′-*O*-dimethyltaxifolin. Tetrahedron Lett. 41, 7925–7928.
Kim, T.Y., Yeo, S.H., Choi, H.S., Kim, J.S., 2011. Patent, Repub. Korean Kongkae Taeho Kongbo, KR 2011088692 A 20110804.
Kook, S.H., Son, Y.O., Chung, S.W., Lee, S.A., Kim, J.G., Jeon, Y.M., Lee, J.C., 2007. Caspase-independent death of human osteosarcoma cells by flavonoids is driven by p53-mediated mitochondrial stress and nuclear translocation of AIF and endonuclease G. Apoptosis 12, 1289–1298.
Krohn, K., Ahmeda, I., John, M., 2009. Enantioselective synthesis of flavan-3-ols using a Mitsunobu cyclization. Synthesis 5, 779–786.
Lee, J.C., Kim, J., Jang, Y.S., 2003. Ethanol-eluted extract of *Rhus verniciflua* stokes inhibits cell growth and induces apoptosis in human lymphoma cells. J. Biochem. Mol. Biol. 36, 337–343.
Lee, S.K., Jung, H.S., Eo, W.K., Lee, S.Y., Kim, S.H., Shim, B.S., 2010. *Rhus verniciflua* Stokes extract as a potential option for treatment of metastatic renal cell carcinoma: report of two cases. Ann. Oncol. 21, 1383–1385.
Muldoon, M.F., Kritchevsky, S.B., 1996. Flavonoids and heart disease. Brit. Med. J. 312, 458–459.
Rakoff-Nahoum, S., 2006. Why cancer and inflammation? Yale J. Biol. Med. 79, 123–130.
Reif, D.W., McCreedy, S.A., 1995. *N*-Nitro-L-arginine and *N*-monomethyl-L-arginine exhibit a different pattern of inactivation toward the three nitric oxide synthases. Arch. Biochem. Biophys. 320, 170–176.
Samoszuk, M., Tan, J., Chorn, G., 2005. The chalcone butein from *Rhus verniciflua* Stokes inhibits clonogenic growth of human breast cancer cells co-cultured with fibroblasts. BMC Complement. Altern. Med. 5, 5.
Sanchez-Tena, S., Fernandez-Cachon, M.L., Carreras, A., Mateos-Martin, M.L., Costoya, N., Moyer, M.P., Nunez, M.J., Torres, J.L., Cascante, M., 2012. Hamamelitannin from Witch Hazel (*Hamamelis virginiana*) displays specific cytotoxic activity against colon cancer cells. J. Nat. Prod. 75, 26–33.
Skehan, P., Storeng, R., Scudiero, D., Monks, A., MaMahon, J., Vistica, D., Warren, J.T., Bokesch, H., Kenney, S., Boyd, M.R., 1990. New colorimetric cytotoxicity assay for anticancer-drug screening. J. Natl. Cancer Inst. 82, 1107–1112.
Son, Y.O., Lee, K.Y., Lee, J.C., Jang, H.S., Kim, J.G., Jeon, Y.M., Jang, Y.S., 2005. Selective antiproliferative and apoptotic effects of flavonoids purified from *Rhus verniciflua* Stokes on normal versus transformed hepatic cell lines. Toxicol. Lett. 155, 115–125.

Sun, C.M., Syu, W.J., Don, M.J., Lu, J.J., Lee, G.H., 2003. Cytotoxic sesquiterpene lactones from the root of *Saussurea lappa*. J. Nat. Prod. 66, 1175–1180.

Ulrich, C.M., Bigler, J., Potter, J.D., 2006. Non-steroidal anti-inflammatory drugs for cancer prevention: promise, perils and pharmacogenetics. Nat. Rev. Cancer 6, 130–140.

Van Rensburg, H., van Heerden, P.S., Bezuidenhoudt, B.C.B., Ferreira, D., 1997. Stereoselective synthesis of flavonoids. Part 4. *Trans*- and *cis*-dihydroflavonols. Tetrahedron 53, 14141–14152.

Wang, W.S., Chen, P.M., Wang, H.S., Liang, W.Y., Su, Y., 2006. Matrix metalloproteinase-7 increases resistance to Fas-mediated apoptosis and is a poor prognostic factor of patients with colorectal carcinoma. Carcinogenesis 27, 1113–1120.

Wiesler, W.T., Nakanishi, K., 1990. Relative and absolute configurational assignments of acyclic polyols by circular dichroism. 2. Determination of nondegenerate exciton coupling interactions by assignment of prochiral aryloxymethylene protons for proton NMR conformational analysis. J. Am. Chem. Soc. 112, 5574–5583.